Fusion Engineering and Design 219 (2025) 115241

Contents lists available at ScienceDirect

Fusion Engineering and Design

journal homepage: www.elsevier.com/locate/fusengdes

Conceptual studies for the EU-DEMO EC heating system transmission line

A. Bruschi [a,*], M. Ciambella [b], D. Dongiovanni [c], F. Fanale [a], P. Fanelli [b], S. Garavaglia [a], T. Glingler [d], S. Marsen [e], T. Pinna [c], P. Platania [a], N. Rispoli [a], A. Salvitti [b], A. Simonetto [a], T. Stange [e], M. Toussaint [f], D. Wagner [g]

[a] Institute for Plasma Science and Technology, National Research Council (ISTP-CNR), Milano, Italy
[b] Department of Economics, Engineering, Society and Business (DEIm), University of Tuscia, Viterbo, Italy
[c] ENEA, Fusion and Nuclear Safety Department, C.R. Frascati, Frascati, Italy
[d] Sapienza University of Rome, Dipartimento di Ingegneria Aeronautica Elettrica ed Energetica (DIAEE), Rome, Italy
[e] Max-Planck-Institute for Plasma Physics, Greifswald, Germany
[f] Ecole Polytechnique Fédérale de Lausanne, Swiss Plasma Center (SPC), Lausanne, Switzerland
[g] Max-Planck-Institute for Plasma Physics, Garching, Germany

ARTICLE INFO

Keywords:
Plasma heating
Electron cyclotron
Quasi-Optical transmission line
Millimeter-waves
Multi-beam mirrors

ABSTRACT

The Electron Cyclotron (EC) Heating system for the EU-DEMO tokamak, designed within the EUROfusion consortium activities as a device to demonstrate the feasibility of a Fusion Reactor, will inject power in different plasma locations to provide a series of tasks, including plasma current ramp-up and ramp-down, central (Bulk) Heating (BH), Neoclassical Tearing Modes (NTM) stabilization, Radiative Instability (RI) control. For fulfilling the tasks, a large amount of mm-wave power at different frequencies has to be generated, transmitted for more than hundred meters, and finally injected into the torus. The transmission line concept being developed is capable to carry multiple frequencies at the same time and can be adapted to final changes of the physics baseline made for optimizing the DEMO performances. The transmission line is arranged in a modular way, in order to be tailored to the final requests of power and reliability, determining the number of gyrotron sources and used ports. The basis of the organization of the system is the "cluster" of sources that share a single multi-beam (MB) transmission line, with one or two clusters sharing the same EC launcher in the equatorial port of DEMO. In this work the basic design and the layout of the transmission line is described, as well as the options for the routing, the MB mirror layout and the grouping in clusters based on reliability calculations. It also describes the work on the broadband polarizers with minimal losses, the coupling of the TEM00 beams to the waveguides, the MB mirror cooling design and the electromagnetic evaluations of transmitted beams to evaluate the coupling losses due to mirror thermal and gravity deformations.

1. Introduction

The EU-DEMO [1], designed within the EUROfusion consortium as a device to demonstrate the feasibility of a Fusion Reactor, is a fusion power plant concept with 2-hours long pulses [2] whose main additional heating system is the Electron Cyclotron (EC) system [3] developed within EUROfusion tasks from early concepts [4,5]. It is in charge of key functions as easing the plasma start-up, sustaining the current ramp-up and assisting the tokamak plasma discharge with heating and stabilization capabilities including the current ramp down assistance at pulse termination. For these tasks it is expected to inject up to 130 MW of power in the plasma [6]. Up to 30 MW are foreseen for Bulk Heating (BH) in plasma center, 30 MW will be launched at the rational surfaces with q=2:1 and 3:2, i.e., at the location of the main Neoclassical Tearing Modes (NTM) in order to stabilise them, while 70 MW will be occasionally needed close to the plasma edge to control Radiative Instability (RI) caused by tungsten particles influx [7]. The development of 2-MW coaxial-cavity multi-frequency gyrotrons as power sources is foreseen [8]. The high number of sources suggest to split them in two RF buildings, which are located at a distance where the maximum external magnetic field of DEMO during the pulse is tolerable by the gyrotrons: in this case the convenient location is at two sides of the Assembly Hall (AH), leaving the AH aperture free for the main components entrance (Fig. 1). In the following, the concepts developed for the DEMO

* Corresponding author.
E-mail address: alessandro.bruschi@istp.cnr.it (A. Bruschi).

https://doi.org/10.1016/j.fusengdes.2025.115241
Received 28 November 2024; Received in revised form 28 March 2025; Accepted 29 May 2025
Available online 12 June 2025

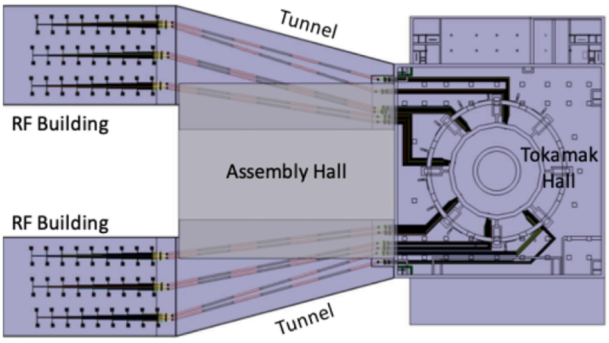

Fig. 1. Top view of RF buildings (left), located at a distance from the DEMO Torus Hall (right) sufficient to prevent source problems due to the tokamak stray magnetic field. The buildings are joint by underground tunnels below the Assembly Hall.

Transmission Line (TL), the first evaluation of losses, for components and routing are described in more details. Finally, the reasons for the choice of the number of sources and ports is addressed.

2. Transmission line concepts

In order to reduce the power losses (a target value is 15 %) and the number of components in the TL, a straight path toward the tokamak building is preferred: it can be realised with wide corridors running partly below the AH. They are connected directly to the RF buildings on one side and to towers connected to the Torus Building (TB) on the other side. The placement of the corridors underground has the advantage of a higher stability of the TL supporting basement, being less sensitive to external accidental loads (wind, snow..) and to internal loads due to the weights of the equipments progressively added in the various buildings. In this straight space about hundred meters long, the distance is covered with Multi-Beam (MB) Quasi-Optical (QO) lines, on the example of W7-X [9], with the advantage of having a relatively small number of components, mainly MB mirrors, to be aligned, cooled and monitored. The MB TL is conveniently enclosed in a metallic envelope to protect the environment from stray microwave radiation and evacuated, to prevent power losses in air and arcing problems, common in W7-X [10]. The choice of a MB QO line is motivated by the reduction of the complexity of the TL system, taking into account the large number of beams to be transmitted, and by a projected reduction of costs when reducing the number of MB mirrors, reported in [4].

Despite the advantages, it is difficult to implement the MB lines in the TB: the need for safely prevent possible contamination of the main TL volume suggests the use of single lines in the TB: circular corrugated waveguides (WG) are foreseen: gate valves at the boundaries between different containment structures (main vacuum, port cell, gallery) allow maintaining individual control of the vacuum of the lines in the TB. The same concept is exploited in the RF building, not for safety reasons in this case but for the reduced space required by a bundle of waveguides (the RF building being crowded with gyrotrons and auxiliary equipments) and for ease of connection and disconnection of single gyrotrons to the main evacuated TL without breaking the MB TL vacuum. The connection between circular corrugated WG to the evacuated MB TL is realized with single-beam mirror pairs, coupling the Gaussian beams, propagating in the QO lines, with the HE_{11} mode propagating in the WG.

One important requirement of the TL is the capability to transmit power with low losses in a certain range of mm-wave frequencies at the same time. Different frequencies are in general required to fulfil the different tasks presented above, since only in this way the power can be deposited efficiently in the different locations of the plasma column. The delivery of the power into the plasma is performed by 4 specialized antennas per launcher, with each launcher located in specific ports of the torus vacuum vessel. Each antenna is made for one or more purposes and designed for specific frequencies. They are not described specifically in this work, and can be found in other published papers [11–13]. For the system presented in this work, 4 independent multi-beam antennas in up to 6 Equatorial ports are foreseen [6].

The presented TL design is instead intrinsically broadband, and only minor adaptations to changes in the frequency range have to be applied, in case adaptations of the main DEMO parameters, as in particular the toroidal magnetic field, are applied. This work focuses on a system capable to transmit power in the frequency range 136–204 GHz, as needed for the DEMO 2018 baseline [14], It can be easily adapted to the transmission of a different range of frequencies, in particular those foreseen for the proposed Low Aspect Ratio DEMO [15], with just a change of the mirror size, adaptation of the RF window thickness and minimal optimization of the mirror surfaces. Given the required number of sources (108 2-MW gyrotrons for the 2018 baseline, assuming 85 % TL efficiency) to guarantee a high reliability of the system [6,11], the TL is organised in 12 clusters of 9 gyrotrons, each cluster using a single MB TL. Two clusters are aiming to a single port (for a total of 6 ports).

More details are given in the following sections: the description starts from the gyrotron sources and ends in front of the launcher, in the port cell of the TH.

3. Transmission line in the RF building

The power generated by gyrotrons, and eventually shaped by a Matching Optic Unit (MOU) at the gyrotron output, is coupled to the HE_{11} hybrid mode propagating into a circular corrugated WG. The chosen WG diameter is 63.5 mm, which is a reasonable compromise between peak power density in the waveguide and mitre-bend mirrors (given the 2 MW per beam it is 24 % higher than the peak power density on the ITER waveguides and mitre-bend mirrors at equal frequency) and alignment errors tolerances (lower with higher WG diameter).

In order to achieve a maximum power coupling efficiency at the transition to the WG (above the 98 % obtained coupling a pure Gaussian beam with an open-ended waveguide), either a beam (from the gyrotron or the MOU) with a high Gaussian TEM00 content (above 98 %) is coupled to a corrugated horn (detailed below), or a pre-formed beam shape with a field closer to the HE_{11} must be produced at the WG input, with a proper shaping of the mirrors in the gyrotron and/or the MOU. The WG are evacuated and can be isolated from the main TL vacuum by means of gate valves, to ease maintenance.

The gyrotrons of a cluster are arranged on a line, with output facing the output of the nearby cluster, in order to form a bundle of 18 parallel waveguides directing towards the TB. In a RF building six clusters are hosted (Fig. 2).

The arrangement of two clusters, including the conditioning loads close to each gyrotron, is shown in Fig. 3. The minimum spacing

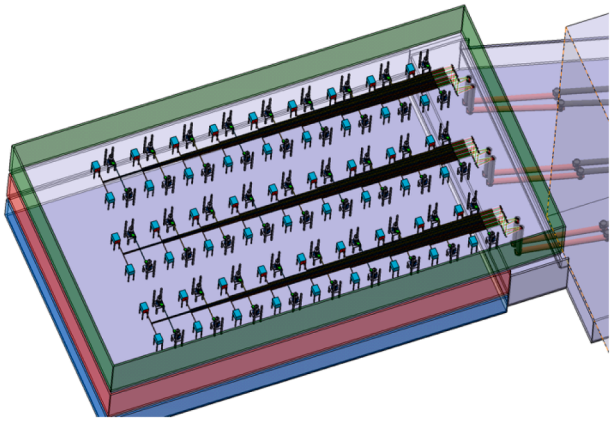

Fig. 2. One of the two RF Buildings, hosting 6 clusters (in total 54 gyrotrons) each. MB TLs are on the right.

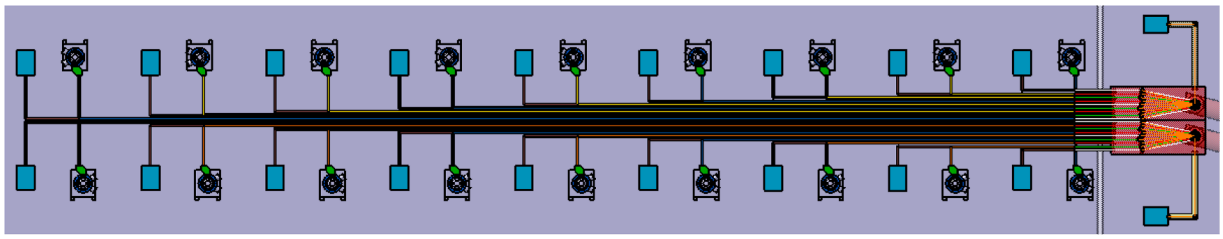

Fig. 3. Two clusters (rows) of gyrotrons with facing outputs, forming a bundle of 18 parallel waveguides. Close to each gyrotron a RF load (light blue) is used for gyrotron conditioning. Another load can be provided close to the MB TL.

between gyrotrons has been set to 7 meters, in order to prevent disturbances on a gyrotron operation by the presence of the magnetic field of a nearby gyrotron.

Individual beams at the exit of the WG (ending with tapers, to maximize coupling with Gaussian beam in space) are directed by a couple of Matching Mirrors (MMs) to a specific location at a lower level, as seen in Fig. 4, where all the beams can be bundled together, and finally combined in a parallel, centered octagonal regular bundle to be inserted in the MB TL. A scheme of the coupling is shown in Fig. 4.

A scheme of the beam trajectories, including the possibility to redirect the beams to a single RF load with the movement of two mirrors (one focusing and the rotatable plane mirror) is shown in Fig. 5.

The sequence of two focusing mirrors is modelled with standard formulas of Quasi-Optical (QO) theory [16], describing Gaussian beam propagation and expansion in free space. The focal lengths are chosen to match the beam size at the WG exit (w_G=20.4 mm) and provide the desired beam waist (w_M=41.5 mm for the present design), equal for all beams, at the combining mirrors placed at the entrance of the MB TL. The two mirrors in the line directed to the load do the matching to the required size for the beam entering the load. The overall design (more details in [6]) is confocal, thus intrinsically broadband [16]. The whole mirror set assembly enclosed in one envelope is under vacuum, without separation to the main TL vacuum. The combining mirrors are plane mirrors placed on three levels, such that the beams are injected in the MB TL with parallel axes at the vertexes of an octagon plus one at the center. Mirrors are packed as close as possible to redirect the nine incident beams downwards, in the direction of the first mirror of the MB TL.

4. Multi-beam transmission line layout

Twelve MB TLs, one for each cluster and grouped by two nearby TLs directed to one specific DEMO port, will run straight in corridors under the AH.

The initial arrangement of the DEMO MBTL is able to transmit nine beams and consists of a Combining Mirror (CM) box above the first focusing mirror (FM1) followed by 6 mirror units with 2 mirrors each (see Fig. 6, top). The last element is again a focusing mirror with the Splitting Mirror (SM) box on top.

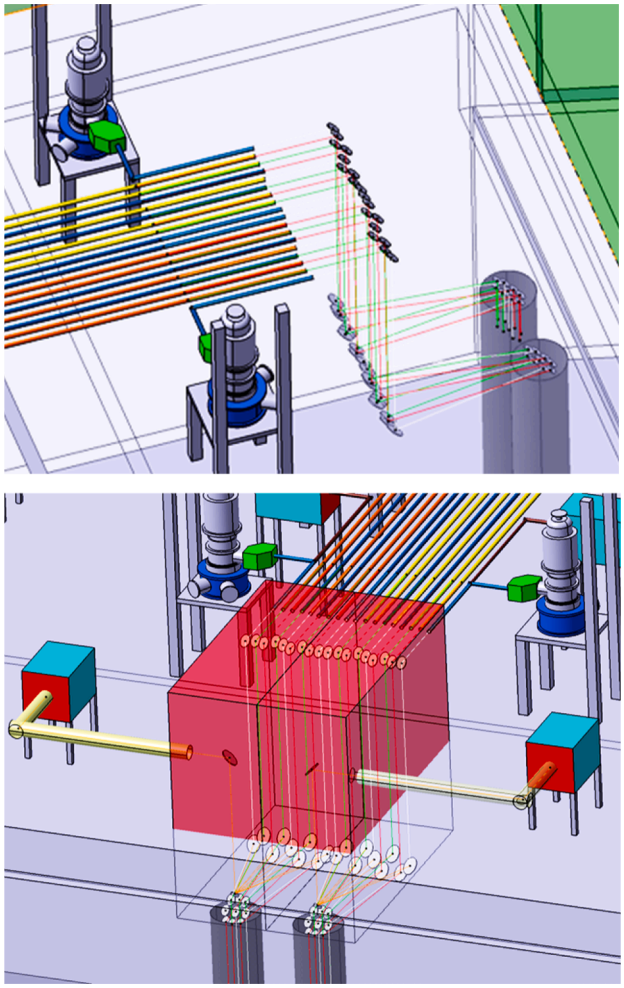

Fig. 4. Top and bottom: views of the matching optics between the WG coming from the gyrotrons and the MB TL towards the TB. At the bottom, a sketch of how the mirrors of two clusters can be enclosed under vacuum (red boxes, max. extension of the enclosure is shown) and a line to an additional load for each cluster can be integrated.

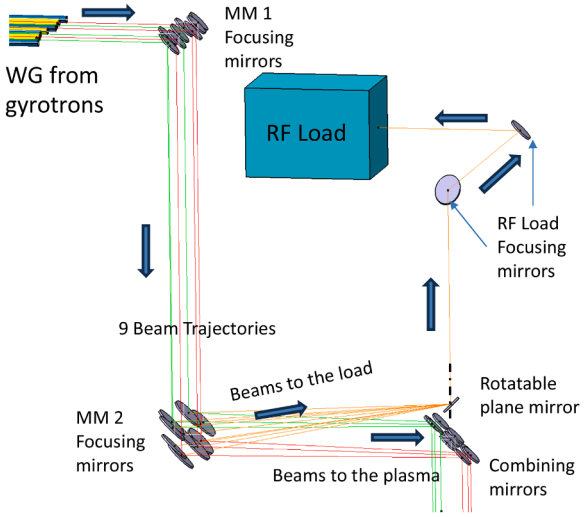

Fig. 5. Path of beam axes from the WGs to the combining mirrors and the alternative path to reach the RF Load The MM2 mirrors are tilted to reach the rotatable and tiltable plane mirror on the top of the combining mirrors assembly. This redirects the beam vertically up towards two focusing mirrors and then into the RF load.

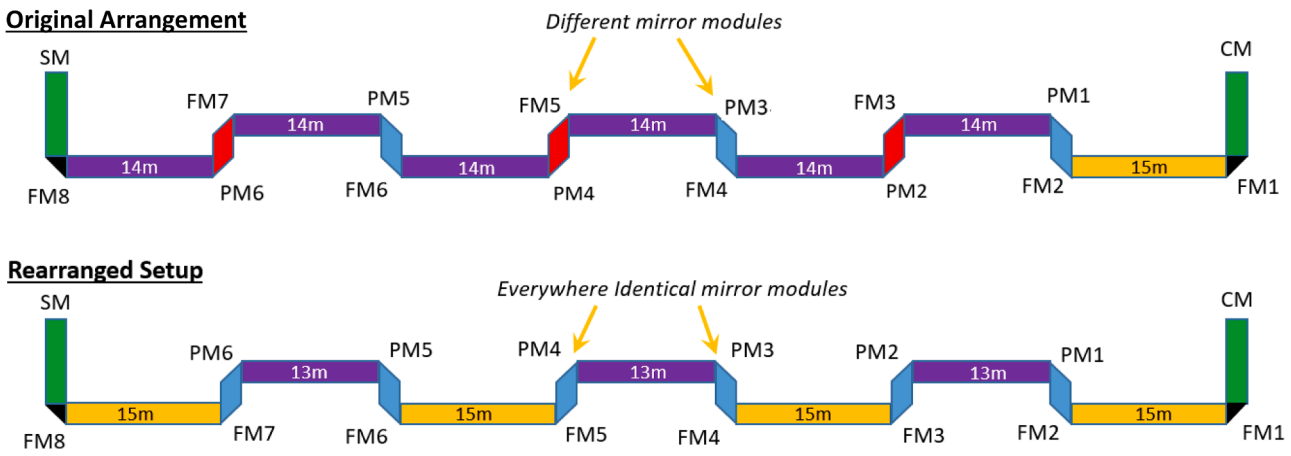

Fig. 6. Setup of the original MB TL presented in [6] (top) and a rearranged setup with some advantages (bottom).

The mm-wave design of each line, made with 8 large focusing mirrors, presented in [6], profits from the work done for the W7-X transmission line, in particular for the choice of the arrangement of the mirrors. In fact, the surface of the multibeam mirrors cannot be matched individually to all beams, which are superimposed on the mirror surface. For this reason, after one or two mirrors the envisaged TEM_{00}-mode is mixed with unwanted higher order modes. In [17], the so called "square arrangement" of four (or multiple of four) confocal mirrors is found suitable for compensating at an optimal level the aberrations arising from the off-axis reflection on mirrors of the Gaussian beams, first described in [18].

The simple idea is to mirror the whole setup and to inject the mix of TEM_{00} and spurious modes again into exactly the same mirror setup (see Fig. 7). The reciprocity theorem promises that the original pure TEM_{00} is mostly recovered. This is also valid for beams with off axis incidence (sketched in Fig. 7 by the additional red arrows). All elements must be on a straight line to keep the symmetry of the imaging from mirror to mirror.

How the "unfolding" of the square configuration can provide a suitable transmission along a line with the addition of plane mirrors is shown in Fig. 8.

The necessary symmetry of the setup is in fact not changed by inserting 2 additional plane mirrors after the second focusing mirror (FM2) and the third focusing mirror (FM3). Fig. 8 shows the resultant MBTL of W7-X, which corresponds to the first half of a single MBTL of DEMO.

Analysis of the alignment method, presently ongoing, shows that a different mirror arrangement has advantages. Fig. 9 shows again the setup of Fig. 8, with an adapted sequence of the mirrors. In alternative to the setup in Fig. 8, a second plane mirror can be inserted right after the first plane mirror. This does not change the symmetric imaging properties, and the resulting transmission line will have the same performance as the version of Fig. 8.

Fig. 6 shows both solutions in comparison.

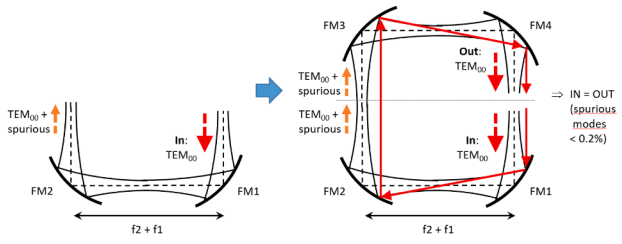

Fig. 7. Square confocal arrangement of 4 focusing mirrors (FM) allows to recover the incident TEM_{00} after four reflections, even though spurious modes are generated in between due to the unmatched mirror surfaces.

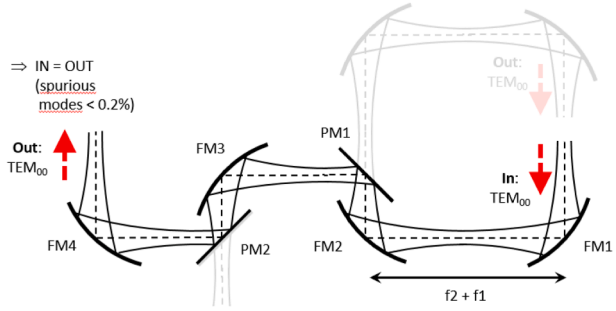

Fig. 8. Insertion of two plane mirrors (PM) into the setup of Fig. 7 to realize a transmission line.

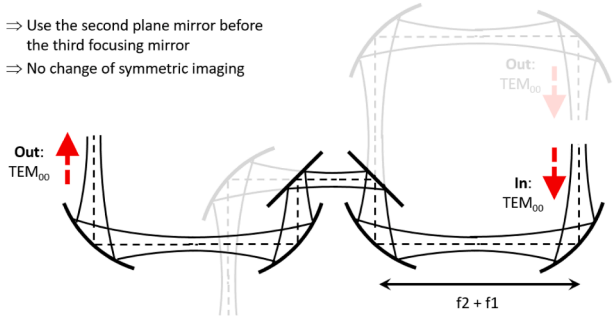

Fig. 9. Insertion of two consecutive plane mirrors (PM) into the setup of Fig. 7 to realize an alternative transmission line.

The advantages of the new setup are as follows:

- The positioning of targets for alignment is more practical on the lower multibeam mirrors.
- Only one type of mirror units is necessary: PM at the top & FM at the bottom. In the current setup we need two different mirror units where the position of FM and PM is swapped.
- Same distance of all top mirrors (13 m) and all bottom mirrors (15 m)
- The procedure to keep symmetry between FMs is potentially easier.

The evacuation of the MBTL enclosure can be performed with pumping stations along the line, but the preferred locations are at the both sides of the MBTL. All the seals on the line should be metallic, or with O-rings protected by metal liners, to prevent loss of tightness due to microwave damage to the elastomers.

5. Multi-beam transmission line evaluation

An off-axis parabolic shape for the mirror surface has been chosen for the simplicity of modelling the beam trajectories, that have parallel and crossing beam axes only for this choice. Also, the results of the modelling showed that the performances of the paraboloid shape are comparable, if not better, than other shapes, as for example the elliptical paraboloid.

The actual design adapted the number of mirrors of each line (must be a multiple of four) to the required distance to cover between the RF building and the TB, taking into account to have a reasonable mirror size. Once chosen the focusing mirror number (8), then the distance between two focusing mirrors is given (15 m.). The mirrors dimensions depend then on the separation of the beam axes and the beam radii on the mirror surface (for the minimum frequency to be transmitted, due to the different beam expansion rate) at the distance between two focusing mirrors. The resulting size of focusing mirrors, compatible with the lower transmitted frequency of 136 GHz is 965 × 1365 mm and for the plane mirrors, where the beams are narrower, is 950 × 1273 mm. The cylindrical enclosure under vacuum needs an internal diameter of 1 m minimum.

Between two focusing mirrors, on which the beams have the maximum size, their axes are alternatively crossing or parallel to each other (see Fig. 10). The MB TL has been modelled with the electromagnetic software GRASP [19], to evaluate the spillover and the coupling losses in the ideal case of undeformed perfectly aligned mirrors.

While results for the initial setup shown in Fig. 6 (top) are given in [6], results for the alternative configuration at the bottom of Fig. 6 are shown in Fig. 11 for the different beams, depending by their position in the octagon with respect to the orientation of the incidence plane. Also in this case, due to the size of the mirrors the spill-over losses are very low, of the order of 0.03 %, while coupling losses are of the order of 0.06 %.

For comparison, the ohmic losses estimated in the MBTL 16 mirrors, assumed with a copper surface and using the polarization with the lowest losses (close to realistic assumption, given the layout), are of the order of 1.5 %.

Non idealities, such as mirror deformation (due to the heat load during pulses and the mirror weight) and misalignments will play a role in the overall losses.

In order to perform a first evaluation of the impact of mirror deformations on the MBTL, deformed parabolic mirror surfaces have been introduced in the GRASP model described above for the original case, taking the deformations as resulting from the thermal-mechanical analysis performed on the mirrors, given the cooling channel geometry, inlet temperature and flow rate, as described in the following section. Very preliminary results are obtained considering the same deformations pattern for each of the 8 focusing mirrors, while the 6 plane mirror surfaces have been considered undeformed, being the plane mirror still not modelled. Preliminary resulting patterns, for undeformed and deformed parabolic surfaces are shown in Fig. 12 for some beams (others are symmetrically deformed).

Coupling losses quantify the deformation of the beam along the transmission line and determine the power fraction remaining in the fundamental gaussian beam centered around the propagated beam axis on the exit plane where the beam waists are expected. In Table 1 the power coupled to the design Gaussian beam and the coupling loss (defined as power not coupled to the design Gaussian beam) are given for the different beams in the case of undeformed and parabolic deformed mirror surfaces. Part of this "lost" power will be transmitted in the matching optics and into the waveguide. The power lost to the TEM00 mode are found around 2.5 %.

Fig. 10. section of the original MB TL between FM5 and PM5 with the beam axes of the 9-mirror crossing between PM4 and FM6.

6. Design of MB mirrors

The initial design of the MB mirror cooling layout, with which the above deformation results were obtained, was a single spiral channel extending from the center to the periphery with a semi-circular section (diameter of 1.2 cm). The chosen materials are 316L (N)-IG stainless steel for the bulk with honeycomb structure at the back and pure copper for the layer 2 mm thick (see Fig. 13). The maximum temperatures reached in pulses are not critical [6], being in an acceptable range even with a single spiral cooling circuit.

A critical consequence of the choice of the cooling layout are the deformations induced by temperature inhomogeneities, not negligible for the beam propagation.

The ohmic load deposited by beams in fact is far from uniform (see Fig. 14 for the reflection of 9 simultaneous beams at 204 GHz, each with Gaussian distribution, with total absorbed power of 20.9 kW).

In Fig. 14 the power is 2 MW for each beam and the absorbed power density on the mirror surface is calculated as $P_{abs}=P_{inc}A$, where A=0.116 % is the absorption coefficient, evaluated assuming 204 GHz, perpendicular polarization (H-plane reflection), and a roughness factor of 1.3 [20]. The thermal analyses were performed with cooling flow rate of 60 l/min.

In order to improve the cooling efficiency and reduce the coupling losses due to deformations, the single spiral of the initial model is replaced with a more efficient double spiral, permitting the split of the flow rates in two parallel channels, reducing also the pressure drop (≤6 bars) and adapting the cross-section to a rectangular shape (Fig. 15). The cooling system has a single inlet and two outlets. With 30 l/min per spiral, a section of ~118 mm^2 (leading to an average velocity of 4.2 m/s) the heat transfer coefficient, supposing to use turbulence promoters (as an artificially increased roughness of ~100 μm) is ~27000 $W/(m^2K)$. The thermal simulations were performed with the ANSYS suite, using Finite Element Method (FEM) approach.

The thermal analysis is in steady state and the structural is static. A preliminary transient thermal simulation showed that the steady-state condition was reached in approximately 50 seconds after the start of the pulse. The temperature results of the steady state thermal simulation are shown in Figs. 16 and 17.

The higher temperatures reached in the spots along the longer axes could be reduced, in future refinements, by increasing locally the flow velocity, with a reduction of the channel section (in particular the channel depth) following the example of the W7-X MB mirrors [21].

Structural analysis is made with boundary conditions:

- Temperature distribution, resulting in thermal expansion, main cause of deformation.
- Pressure inside the channel due to water: $p_{water} = 10\ bar$ (conservatively constant).
- Forces in inlet and outlet to represent the continuity of the flow.
- Standard Earth Gravity, considering both parabolic mirrors placed at top and bottom.

The maximum total deformation is 0.068 mm, found at the edges of the bottom mirror (Fig. 18). The difference between the configurations is the effect of the gravity on the 45° mirror. Gravity in combination with other loads is worse in the case of the bottom mirror. The main contribution to the total deformation comes from the thermal load.

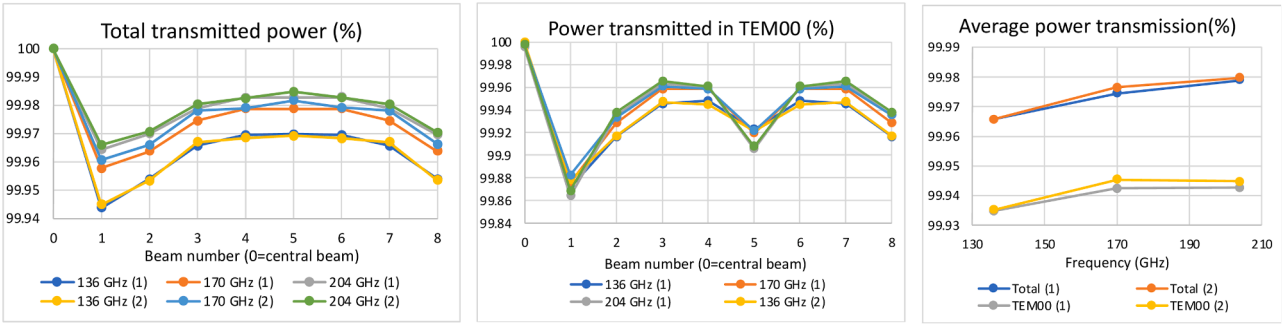

Fig. 11. Left: Transmitted power fraction along the MBTL for ideal Gaussian beams at the input (beams are numbered from 0 o 8), as from the model in GRASP [19]. The complement to 1 is the fraction lost for spillover. Center: Fraction of the power transmitted in TEM_{00} mode. The complement to 1 is the fraction lost for spillover and converted to higher order modes. Right: Comparison of the average power transmission fraction for the different frequencies.

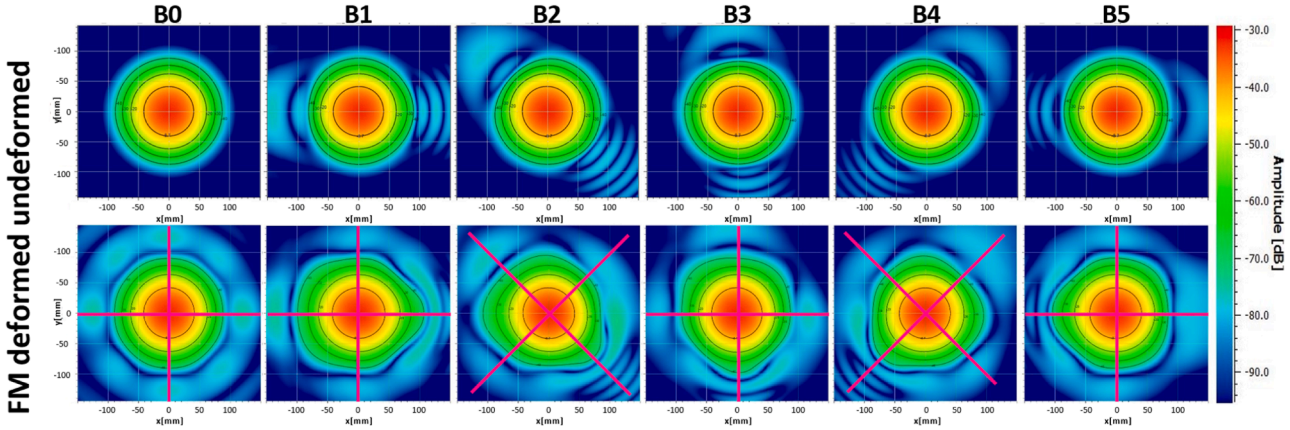

Fig. 12. Patterns of radiation at the exit of the MB TL in the ideal case of aligned and undeformed mirrors and ideal input Gaussian beams, and in the case of FM deformed mirror surfaces, from beam 0 at the left to beam 5 at the right. For each beam, the quantity represented in the plots is the |E| on a plane grid at the exit of the MBTL; the contours are shown by solid lines at -8.7, -20, -30, -40 dB with respect to the peak power.

Table 1
Percentage of power coupled to the TEM00 mode and the coupling losses at the end of the MB TL for the different beams, in the ideal case of aligned and undeformed mirrors and ideal input Gaussian beams, according to the model implemented in GRASP and in the case of deformed focusing mirror (FM) surfaces.

Beam	Coupled power (%)		Coupling losses (%)	
	undeformed	deformed FM	undeformed	deformed FM
0	100	99.374	0.000	0.626
1	99.872	96.405	0.128	3.595
2	99.916	97.354	0.084	2.646
3	99.945	98.059	0.055	1.941
4	99.948	97.274	0.052	2.726
5	99.923	96.099	0.077	3.901
6	99.948	97.089	0.052	2.911
7	99.945	97.981	0.055	2.019
8	99.916	97.437	0.084	2.563

While it is possible that the mirror deformations in the first seconds of the pulse reach a maximum value higher than at the steady state, for such long pulses we focus the attention on the static structural result. Specific transient analyses will be performed on the final design.

With the deformation resulting from this thermal analysis (Fig. 18), the GRASP model of the straight line of 8 parabolic mirrors described above will be run.

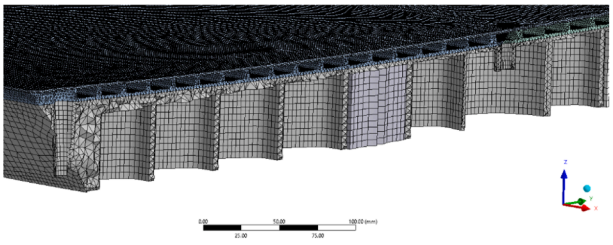

Fig. 13. Cutout of the 50 mm SS honeycomb bulk.

7. Mirror alignment, support and enclosure

The mirror first alignment, foreseen with laser beams, reference surfaces machined on mirrors and low-power mm-wave targets monitored with IR cameras, is made with the line in open air. Proposed adaptation to mirror geometry is the presence of planar surfaces at the mirror sides in order to mount levels, suggesting the rearrangement of beam positions on the mirror, as in Fig. 19.

The vacuum enclosure of the whole line is realized with cylindrical tube sections with the use of metallic gaskets. Needed components are: mounting equipment for IR cameras and inspection ports for inserting targets and checking laser alignment (Fig. 20).

The whole MB TL enclosure, being a large vacuum chamber extending from the gyrotron hall to the TB, has been studied for proper positioning and stable mounting of mirrors. Special solutions are considered, as the use of embedded plates in the basement concrete

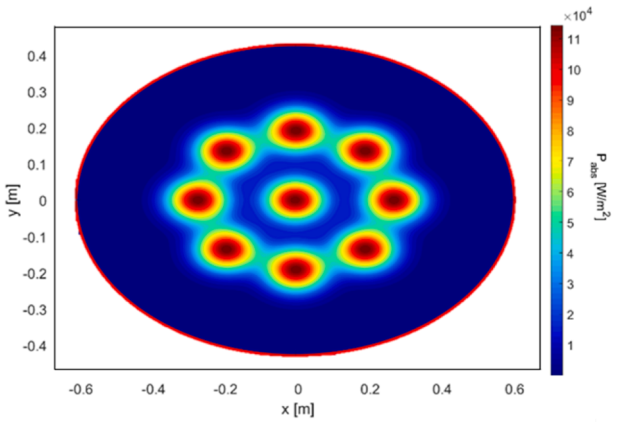

Fig. 14. Thermal load on the parabolic mirror, with maximum above 110 kW/m^2.

(Fig. 21), the sliding plates for fine alignment of mirror towers, adjustable mirror supports less sensitive to the bending of the vacuum enclosures when evacuated. The supports of the top mirror are in fact fixed on the top flange as close as possible to the main cylinder, in order to minimize the mirror displacement when the flange is subject to the atmospheric pressure. The cylinder itself is stiff enough to sustain the mirror weight and resist to off-normal events. A preliminary structural analysis showed the sufficient rigidity of the cylinder but the need to increase the stiffness of the bottom plate and the adjustable feet.

In particular, the use of (manual) hexapod-like mountings is being considered. The main advantages are:

- Optimal access at the mirror center, for water inlet.
- Cheap and simple solution for the mirrors to be aligned.
- Easy to build, no accuracy needs during manufacture.

One difficulty could be in the alignment operations, given the 6 degrees of freedom (offset and tilt are mixed).

In order to check that the alignment of the mirrors is kept during time, a laser alignment system is also possible, with optical polishing of special areas of the mirror surface. This could be useful also to restore the alignment of the MBTL (recovering tilts and offsets on the splitting mirrors) if long-term movements are occurring, but require laser spot position sensors and remotely movable hexapods.

The pumping system should maintain the desired pressure of around 10^{-5} mbar in the large volume. The tightness of the MB TL enclosure is the use of elastic spring-loaded metallic seals and bellows or expansion joints in specific locations to absorb the envelope thermal expansion.

8. Beam splitting unit, tapers and polarizers

At the end of the MB TL, close to the TB wall, the beam bundles are split in single lines, coupled to the WG lines running in the TB Gallery. The matching is accomplished by a symmetrical optical system at the exit of the MBTL, with the addition of polarizing mirrors, in order to provide the correct polarization in the plasma (Fig. 22).

As for the single line at the input of the MBTL, also at the output the alignment of mirrors is foreseen before evacuation, using microwave absorbers as targets.

Broadband polarizers are studied [6] with the aim of reducing losses

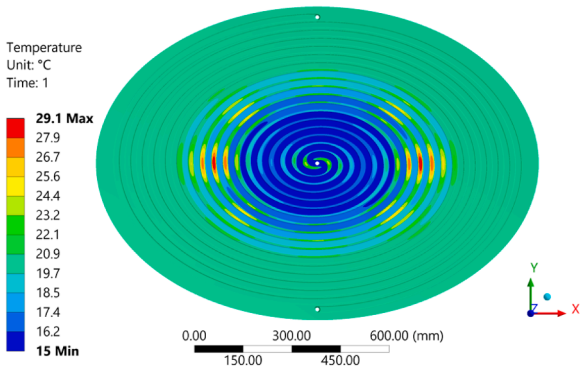

Fig. 16. Temperature of the AISI316 mirror bulk.

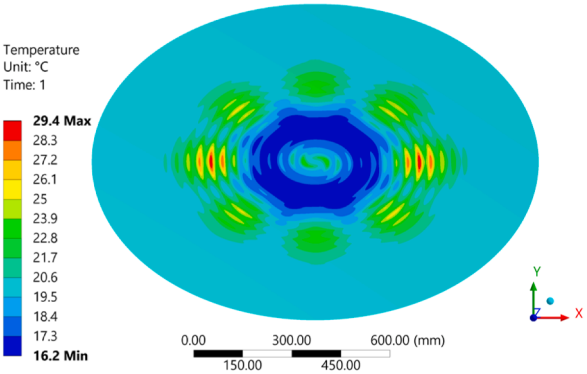

Fig. 17. Copper surface layer temperature.

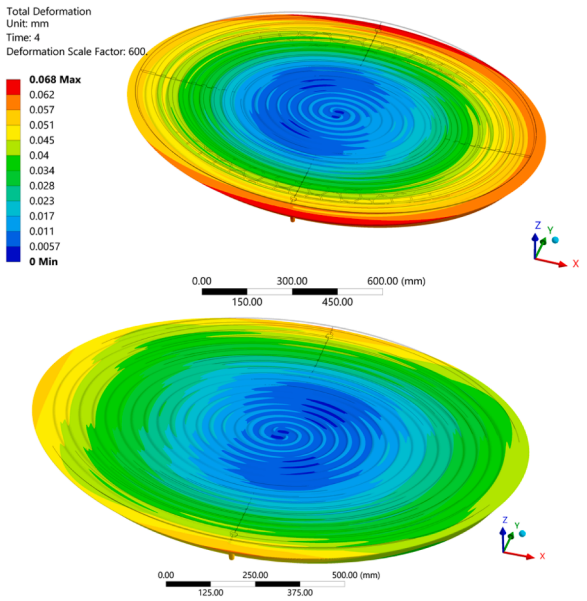

Fig. 18. Deformations of mirrors placed at bottom (top) and top (bottom) of the towers.

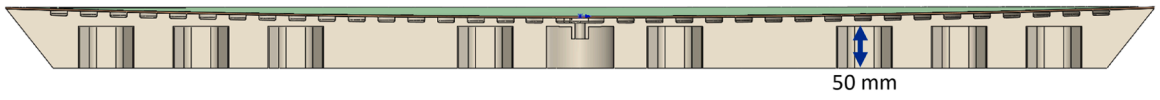

Fig. 15. Two spiral channels below 2 mm copper surface.

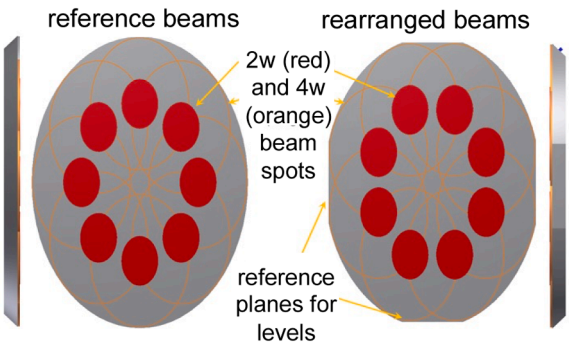

Fig. 19. Alignment eased by planar surfaces on mirrors.

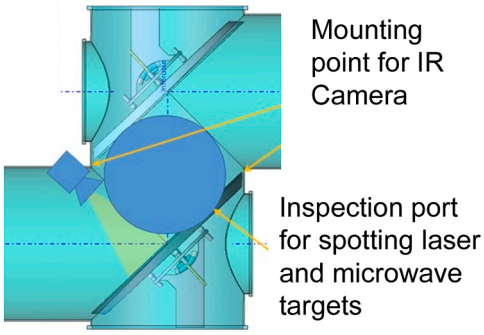

Fig. 20. First alignment eased by enclosure adaptations.

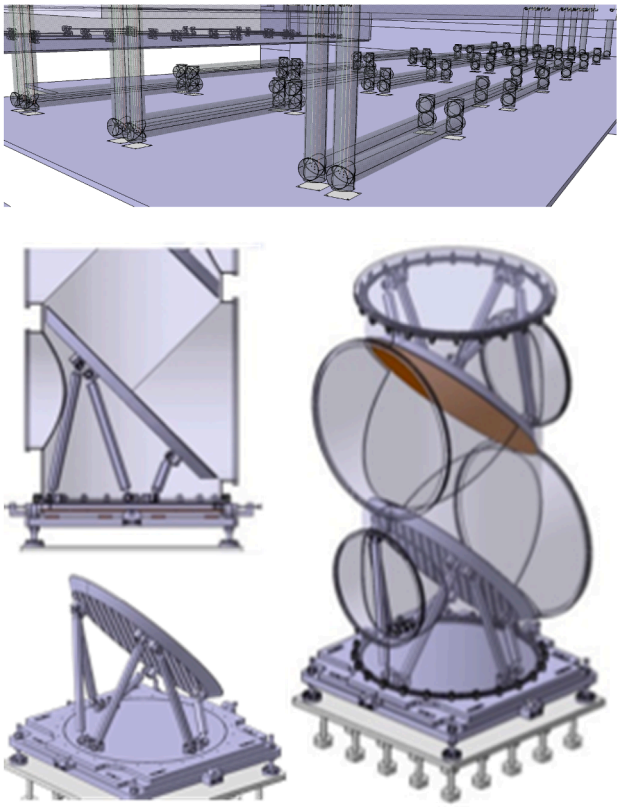

Fig. 21. Top: MB TL mirror towers positioned on plates embedded in concrete. Mid and bottom: MB TL towers and mirror support concept with sliding xy table and manual hexapods.

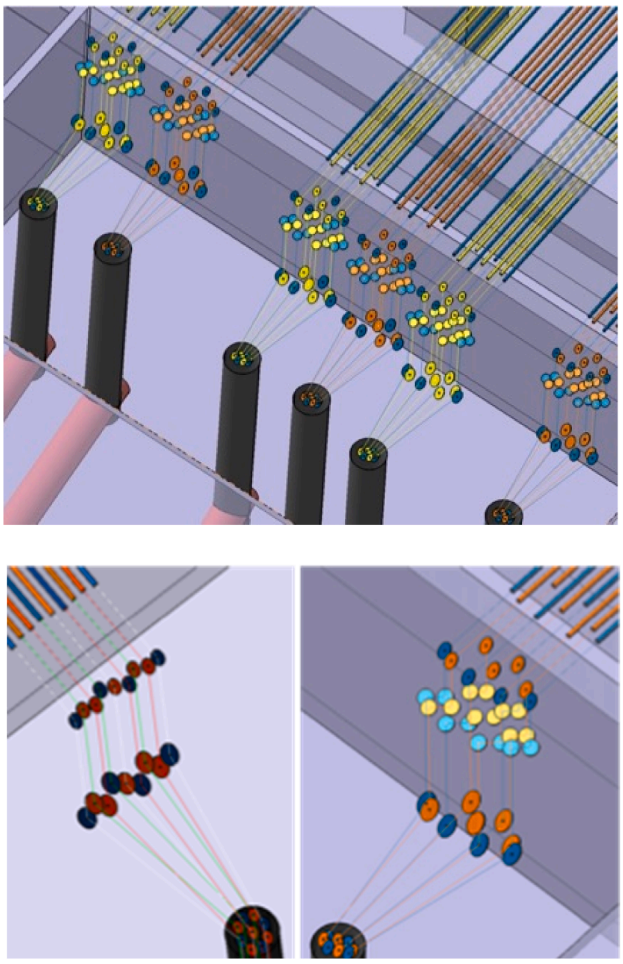

Fig. 22. Top: Optical units for beam splitting and polarization conditioning at the end of the MB TL: the beams are coupled to parallel waveguides traversing the TB wall. Bottom: scheme of the optics at input (left) in comparison with the one at output (right) of the MBTL, showing the addition of two polarizing mirrors (light blue and light yellow) per line. The beam trajectories are shown as thin lines.

with the model developed in [22].

The coupling between the Gaussian free-space beam and the HE_{11} eigenmode of the corrugated waveguide can be improved by using corrugated hyperbolic horns [23] at the input and the output of the waveguide line. For our line, broadband tapers adapting the TEM_{00} to the HE_{11} mode at multiple frequencies are evaluated with mode-matching calculations. Very-low sidelobes and high coupling can be obtained with hyperbolic profile (Fig. 23 and Table 2).

Table 2 shows that the coupling from an open-ended corrugated waveguide to a free-space Gaussian beam can be improved from ~98 % to almost 100 % at the center frequency using such a hyperbolic horn antenna. The calculations also result in a high Gaussian content of the output beam in a wide frequency range.

9. Routing in the torus building

The evacuated WGs path from wall of TB to EC ports is described in [6]. A different version has been studied in order to ease remote maintenance (Fig. 24).

This is true in particular in case of use of alternatives solutions [24] for simplifying the mounting of the very crowded transmission line in the port cell (Fig. 25), that must leave space for the extraction of the port plug hosting the plasma-facing mirrors, for their periodic maintenance: this is shown in Fig. 25 at the left of the WGs entering in the launcher

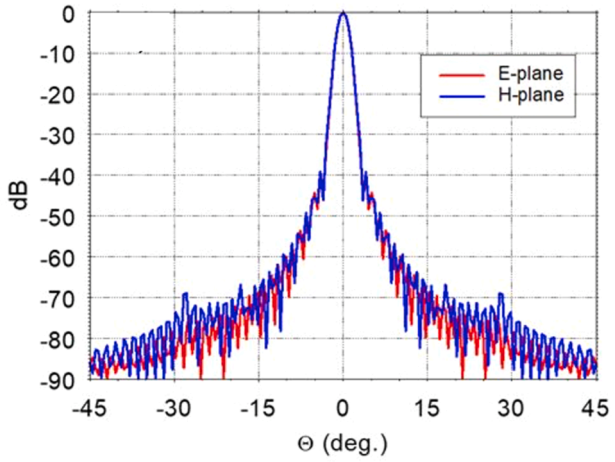

Fig. 23. Calculated far field radiation pattern of the considered hyperbolic horn at 170 GHz with HE_{11} as input mode.

Table 2
Calculated values for the beam radius at the output aperture of the hyperbolic horn w_{out}, the Gaussian beam content η and the beam waist position when assuming radiation out of the open-ended corrugated waveguide with radius 31.75 mm and $w_0 = 20.43$ mm.

frequency	136 GHz	170 GHz	204 GHz
w_{out}	30.36 mm	27.55 mm	25.31 mm
η	99.896 %	99.996 %	99.962 %
z_w	653.99 mm	672.63 mm	652.7 mm

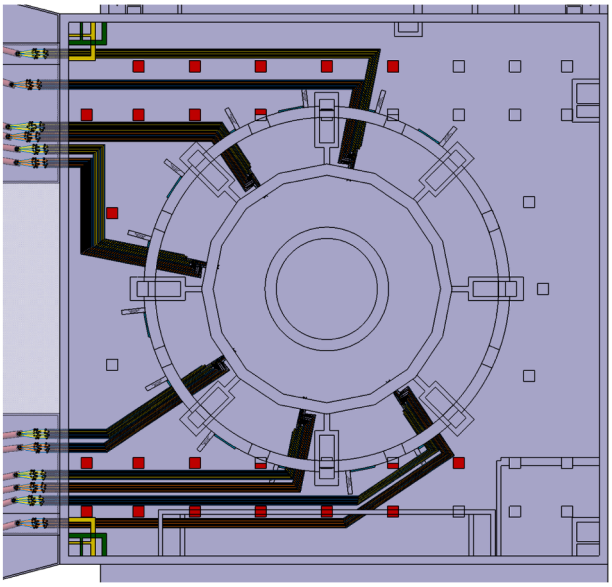

Fig. 24. Alternative routing of WGs in the TB Gallery.

closure plate.

10. TL reliability calculations

RAMI analysis of TLs has been carried out by Fault Trees and Reliability Block Diagram models on the basis of single component fault statistics.

Failure rate data have been retrieved from the Fusion Component Failure Rate Database which consists of component failure models based on historical data of existing fusion facilities and other industrial applications [25]. The TL system has been hierarchically divided into basic components and a Failure Mode Effect Analysis has highlighted failure modes and maintenance activities to be considered in the availability model.

The duty cycle considered is an ideal 70-day plasma operation periods interfaced with scheduled maintenance periods of one week (Ex-vessel maintenance) and four months (Tokamak maintenance). Restoration factor of components subject to preventive maintenance is fixed to 10 %. Corrective maintenance (CM) activities on the TL components located in the ECRH building or in the assembling hall have been considered between 3 days and 1 week according to the complexity of the equipment and of the maintenance activity. Components subject to CM have a restoration faction equal to 100 % (i.e., the component is completely replaced) or 20 % according to the type of component. Other relevant assumptions are associated with the system reliability-wise layout. The first assumption considers that at least six out nine gyrotrons per cluster and related TLs are required to successively inject energy into the plasma. Instead regarding the launchers at least five out of the six ports shall correctly operate to consider the whole ECRH system available.

Results in term of mean inherent availability in 1, 10, 20 years of operations, are 97.8 %, 91.0 %, 88.7 %. A parametric study considered the variability of the duration of maintenance activities. With duration of corrective maintenance of 1 week to 1 month, instead of 3 days – 1 week, availability decreases in 1, 10 and 20 years to 97.0 %, 88.5 % and 85.3 % respectively.

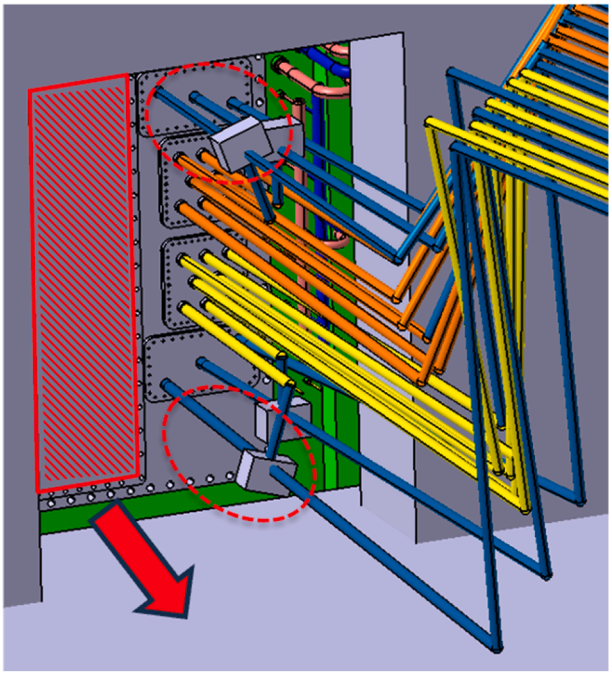

Fig. 25. Present layout of waveguides in the port cell, showing a limited space for the extraction of the port plug, in the direction of the red arrow. This can be eased with alternative solutions proposed in [23].

11. Conclusions

The design of EU-DEMO EC transmission line at conceptual stage is addressing the main challenges: high-power transmission with good efficiency, low losses and high reliability. Improvements on the mirror design, supports and their analysis in non-ideal cases including thermal and other deformation effects are addressed with EM modelling.

CRediT authorship contribution statement

A. Bruschi: Writing – review & editing, Writing – original draft, Supervision, Methodology, Conceptualization. **M. Ciambella:** Formal analysis. **D. Dongiovanni:** Writing – review & editing, Methodology, Formal analysis, Conceptualization. **F. Fanale:** Writing – review & editing, Investigation. **P. Fanelli:** Methodology, Formal analysis, Conceptualization. **S. Garavaglia:** Writing – review & editing, Investigation, Formal analysis, Conceptualization. **T. Glingler:** Investigation, Formal analysis. **S. Marsen:** Writing – review & editing, Investigation, Conceptualization. **T. Pinna:** Writing – review & editing, Formal analysis, Conceptualization. **P. Platania:** Writing – review & editing, Investigation, Formal analysis, Conceptualization. **N. Rispoli:** Investigation, Conceptualization. **A. Salvitti:** Writing – review & editing, Investigation, Formal analysis, Conceptualization. **A. Simonetto:** Investigation, Formal analysis, Conceptualization. **T. Stange:** Writing – review & editing, Methodology, Investigation, Conceptualization. **M. Toussaint:** Writing – review & editing, Investigation, Formal analysis, Conceptualization. **D. Wagner:** Writing – review & editing, Investigation, Formal analysis, Conceptualization.

Declaration of competing interest

The authors declare that they have no known competing financial interests or personal relationships that could have appeared to influence the work reported in this paper.

Acknowledgments

This work has been carried out within the framework of the EUROfusion Consortium, funded by the European Union via the Euratom Research and Training Programme (Grant Agreement No 101052200 — EUROfusion). The Swiss contribution to this work has been funded by the Swiss State Secretariat for Education, Research and Innovation (SERI). Views and opinions expressed are however those of the author(s) only and do not necessarily reflect those of the European Union, the European Commission or SERI. Neither the European Union nor the European Commission nor SERI can be held responsible for them.

Data availability

Data will be made available on request.

References

[1] G. Federici, et al., The EU DEMO staged design approach in the pre-concept design phase, Fusion Eng. Des. 173 (2021) 112959.
[2] M. Siccinio, et al., Impact of the plasma operation on the technical requirements in EU-DEMO, Fusion Eng. Des. 179 (2022) 113123.
[3] M.Q. Tran, et al., Status and future development of Heating and Current Drive for the EU DEMO, Fusion Eng. Des. 180 (2022) 113159.
[4] G. Granucci, et al., Conceptual design of the EU DEMO EC-system: main developments and R&D achievements, Nucl. Fusion 57 (2017) 116009.
[5] S. Garavaglia, et al., EU DEMO EC equatorial launcher pre-conceptual performance studies, Fusion Eng. Des. 156 (2020) 111594.
[6] A. Bruschi, et al., Conceptual design of a modular EC heating system for EU-DEMO, Nucl. Fusion 64 (2024) 106003.
[7] G. Federici, et al., Overview of the DEMO staged design approach in Europe, Nucl. Fusion 59 (2019) 066013.
[8] J. Jelonnek, et al., Design considerations for future DEMO gyrotrons: A review on related gyrotron activities within EURO fusion, Fusion Eng. Des. 123 (2017) 241–246.
[9] W. Kasparek, et al., Status of the 140 GHz, 10 MW CW transmission system for ECRH on the stellarator W7-X, Fusion Eng. Des. 74 (2005) 243–248.
[10] H.P. Laqua, et al., High-performance ECRH at W7-X: experience and perspectives, Nucl. Fusion 61 (2021) 10600.
[11] T. Franke, et al., Integration concept of an electron cyclotron system in DEMO, Fusion Eng. Des. 168 (2021) 112653.
[12] P. Spaeh, et al., Design progress of structural components of the EU DEMO EC equatorial launcher, IEEE Trans. Plasma Sci. (2024), https://doi.org/10.1109/TPS.2024.3353822.
[13] C.M. Borderas, et al., Pre-conceptual design of the fixed mirrors for the DEMO Electron Cyclotron Heating antenna, Fusion Eng. Des. 199 (2024) 114139, https://doi.org/10.1016/j.fusengdes.2023.114139.
[14] M. Siccinio, et al., Development of the plasma scenario for EU-DEMO: status and plans, Fusion Eng. Des. 176 (2022) 113047.
[15] C. Bachmann, et al., Re-design of EU DEMO with a low aspect ratio, Fusion Eng. Des. 204 (2024) 114518.
[16] P.F. Goldsmith, Quasioptical Systems, Wiley-IEEE Press, Springer US, 1998.
[17] L. Empacher, W. Kasparek, Analysis of a multiple-beam waveguide for free-space transmission of microwaves, IEEE Trans. Antennas Propag. 49 (2001) 483–493.
[18] J.A. Murphy, Distortion of a simple Gaussian beam on reflection from off-axis ellipsoidal mirrors, Int. J. Infrared Milli. Waves 8 (1987) 1165–1187, https://doi.org/10.1016/1350-4495(95)00047-X.
[19] GRASP Technical Description 2017 TICRA (www.ticra.com) Knud Pontoppidan.
[20] W. Kasparek, et al., Measurements of ohmic losses of metallic reflectors at 140 GHz using a 3-mirror resonator technique, Int. J. Infrared Milli. Waves 22 (2001) 1695–1707.
[21] H. Hailer, et al., Mirror development for the 140 GHz ECRH system of the stellarator W7-X, Fusion Eng. Des. 66/68 (2003) 639–644.
[22] D. Wagner, et al., Minimization of the ohmic loss of grooved polarizer mirrors in high-power ECRH systems, J. Infrared Milli. Terahz Waves 38 (2017) 191–205.
[23] M.A. Shapiro, R.J. Temkin, Calculation of a hyperbolic corrugated horn converting the TEM00 mode to the HE11 mode, J. Infrared Milli. Terahz Waves 32 (2011) 283–294.
[24] D. Birlan, et al., Conceptual design proposal for the EU-DEMO electron cyclotron ex-vessel waveguide system with enhanced remote maintainability This volume.
[25] T. Pinna, et al., Fusion component failure rate database (FCFR-DB), Fusion Eng. Des. 81 (2006) 1391–1395.